Thermal island destabilization and the Greenwald limit

R.B. White, D.A. Gates, D.P. Brennan[1]

[1]*Plasma Physics Laboratory, Princeton University,*

P.O.Box 451, Princeton, New Jersey 08543

(Dated: January 15, 2015)

Abstract

Magnetic reconnection is ubiquitous in the magnetosphere, the solar corona, and in toroidal fusion research discharges. In a fusion device a magnetic island saturates at a width which produces a minimum in the magnetic energy of the configuration. At saturation the modified current density profile, a function of the flux in the island, is essentially flat, the growth rate proportional to the difference in the current at the O-point and the X-point. Further modification of the current density profile in the island interior causes a change in the island stability and additional growth or contraction of the saturated island. Because field lines in an island are isolated from the outside plasma an island can heat or cool preferentially depending on the balance of Ohmic heating and radiation loss in the interior, changing the resistivity and hence the current in the island. A model of island destabilization due to radiation cooling of the island is constructed, and the effect of modification of the current within an island is calculated. An additional destabilization effect is described, and it is shown that a small imbalance of heating can lead to exponential growth of the island. A destabilized magnetic island near the plasma edge can lead to plasma loss, and because the radiation is proportional to plasma density and charge, this effect can cause an impurity dependent density limit.

PACS numbers: 52.25.Fi, 52.25.Gj

I. INTRODUCTION

Magnetic islands in fusion devices are practically never in a state of linear growth. At very small width the linear analysis is no longer correct, and the island evolves through states of stable saturation depending on varying equilibrium parameters and local current density changes. Because of this the magnetic field configuration can be followed on a slow time scale. At saturation the modified current density profile, a function of the perturbed helical flux, is essentially flat in the island. Further modification of the current density profile in the island interior by current drive, bootstrap current, or other effects causes additional growth or shrinking of the saturated island. Because the island is to some degree thermically isolated from the outside plasma, with heat flowing primarily past the island in the vicinity of the X-point[1], heat from the plasma center does not easily penetrate the island and an island can heat or cool preferentially depending on the internal balance of Ohmic heating and radiation loss. The modified temperature changes the internal current magnitude and the saturated island width. Cooling, and thus an increase in the resistivity and a decrease in the current in the island interior is destabilizing, and heating is stabilizing[2]. This effect has been hypothesized as being responsible for the Greenwald limit on plasma density in tokamaks[3–7].

In section II we review the local analysis of island formation and saturation. In section III island destabilization due to current perturbation is constructed, including an additional destabilizing term due to island asymmetry[8]. In section IV the temperature inside the island is calculated due to a balance of Ohmic heating and radiation loss, and it is shown that heating causes island saturation at a small width, but heat loss due to radiation can cause exponential growth. We show that the dominant equilibrium parameter determining the saturated width of a magnetic island is in fact the internal island temperature. In section V we examine a method of constructing, for the purposes of island saturation and evolution, a cylindrical equilibrium approximating any given equilibrium of arbitrary aspect ratio or shape. In section VI are the conclusions.

We use a large aspect ratio approximation, with a simple circular equilibrium. Use cylindrical geometry r, θ with a conducting wall at the minor radius $r = 1$. Model profiles[9]

are given by the form of the current density profile

$$j(r) = \frac{j(0)}{[(1 + (r/r_0)^{2\nu}]^{1+1/\nu}}, \tag{1}$$

with the associated field helicity given by

$$q(r) = q(0)[(1 + (r/r_0)^{2\nu}]^{1/\nu}, \tag{2}$$

and also $j(0) = 2/q(0)$ and

$$q(r) = \frac{r^2}{\int_0^r j(r) r dr}. \tag{3}$$

The constant r_0 gives the width of the current channel and profiles with $\nu = 1, 2, 4$ are refered to as peaked, rounded, and broad. In section V we will generalize the treatment to arbitrary equilibria taken from either experimental data or fully toroidal simulations.

With the magnetic field normalized to 1 at the magnetic axis $r = 0$, and constant across the plasma cross section, the toroidal flux is $\psi_t = r^2/2$, and the poloidal flux is $\psi_p = \int dr r/q(r)$. The helical flux associated with a single mode with toroidal and poloidal harmonics given by n, m is given by $\psi = \psi_p - (n/m)r^2/2$.

Introduce a single magnetic island with $m \geq 2$ caused by a perturbation of the helical flux given by[10, 11]

$$\psi(r, \theta) = \psi_0(r) + \psi_1(r) cos(m\theta), \tag{4}$$

and similarly for the current density. The current density profile is related to the helical flux through $j = \nabla_\perp^2 \psi + 2n/m + \delta j$, where δj is a modification of the current in the island due to applied localized current or modification of the plasma resistivity in the island interior, and $\nabla_\perp^2 \psi_1 = \psi_1'' + \psi_1'/r - m^2 \psi_1/r^2$. An example of the unperturbed helical flux is shown in Fig. 1, with vanishing derivative at the rational surface $q(r_s) = m/n$. When the island width is larger than the tearing layer the inertia is negligible[12] and the current density is a function of the perturbed flux, $j = j(\psi)$. The solution to the perturbed flux outside the island is then given to lowest order in the magnitude of ψ_1 by

$$\nabla_\perp^2 \psi_1 = \frac{dj}{d\psi_0} \psi_1 + \delta j_1. \tag{5}$$

Since this equation has a regular singular point at $r = r_s$ it must be integrated using boundary conditions at $r = 0$, where $\psi_1 \sim r^m$ and at the conducting boundary $r = 1$, where

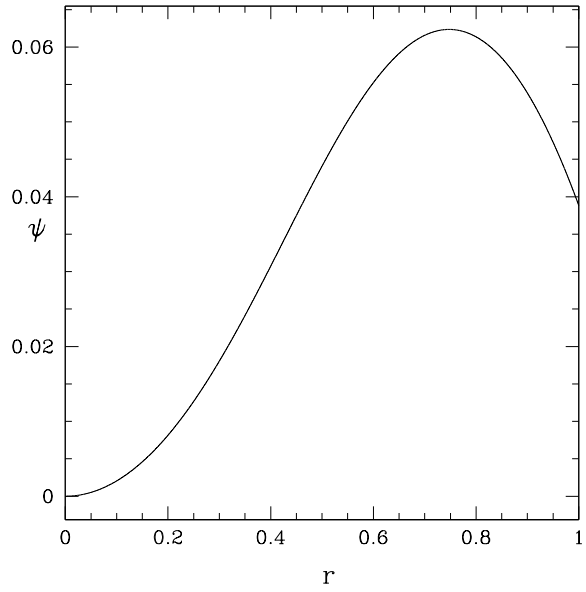

FIG. 1: Equilibrium helical flux.

$\psi_1 = 0$, and matched at $r = r_s$, where the derivatives are singular. The modification due to an additional current density within the island δj can be treated perturbatively.

Analysis of a general situation is accomplished by numerical integration using a fourth order Runge Kutta scheme. In Fig. 2 is shown the perturbed flux and its derivative for a fairly peaked current profile, $r_0 = 0.548$, $\nu = 1.53053$, $q(0) = 0.9$, $r_s = 0.7288$. This profile is chosen to approximately match conditions prior to a density limit disruption[4], and we will refer to it as the disruption test case. It is slightly above the $m = 2$ tearing mode instability threshold. Simulations with a fully time dependent code including heat transport[13] were carried out with a slightly different equilibrium because of the need to avoid the $q = 1$ surface. Comparison with those simulations is discussed in section V.

The perturbed flux $\psi_1(r)$ is integrated from the boundaries at $r = 0, 1$ up to near the rational surface r_s so subtracting the limiting values of ψ_1' for $r \to r_s+$ from that for $r \to r_s-$ gives the value of Δ' for the linear mode. For purposes of plotting these results we normalize the perturbed flux $\psi_1(r)$ to 1 at the rational surface. An actual mode in a device has amplitude α typically smaller than 10^{-3}.

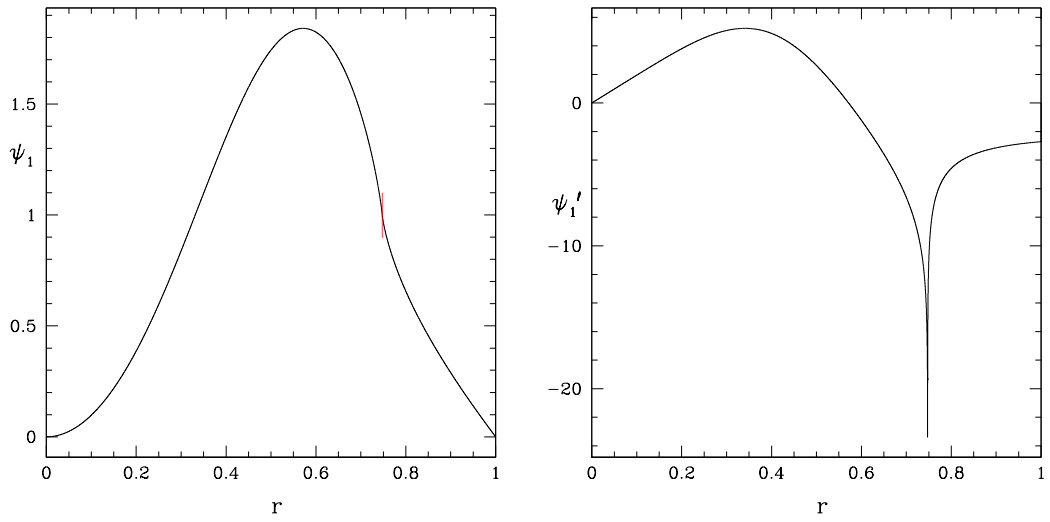

FIG. 2: The perturbed helical flux $\psi_1(r)$, and the derivative $\psi_1'(r)$.

II. LOCAL ANALYSIS

Let $r = r_s + x$. Near the rational surface, expanding $\psi = \psi_0(r) + \psi_1(r)cos(m\theta)$ about the rational surface and $m\theta = \pm\pi$ we have

$$\psi(r,\theta) \simeq \psi_0(r_s) + \psi_0''(0)\frac{x^2}{2} + \psi_1(r_s)\left(-1 + \frac{d\theta^2}{2}\right) \tag{6}$$

and since $\psi_0''(0) < 0$ this equation is hyperbolic with an X-point at $x = d\theta = 0$ and the separatrix value of ψ is $\psi_s = \psi_0(r_s) - \psi_1(r_s)$. The elliptic point is at $x = 0$ and $m\theta = 0$.

We also have $\psi_0 \simeq \psi_0''(0)x^2/2$ and $\nabla_\perp^2\psi_1 \simeq \psi_1''$ so Eq. 5 without a current perturbation becomes $\psi_1'' = k\psi_1/x$ with $k = (dj/dx)/\psi_0''$. The asymptotic solution for small x with $\delta j = 0$ is, including the first three terms

$$\begin{aligned} \psi_1 &= \psi_1(0)[1 - Ax + kxln(-x)], \quad x < 0 \\ \psi_1 &= \psi_1(0)[1 - Bx + kxln(x)], \quad x > 0. \end{aligned} \tag{7}$$

Boundary conditions at $r = 0$ and $r = 1$ and the matching of these two functions determines $\psi_1(r)$ within overall normalization. The constants A, B (normally positive) are determined by integrating Eq. 5 using the boundary conditions at $r = 0, 1$. Note that because of the logarithms the derivatives are singular at the rational surface.

We then have also to this order

$$\psi_1' = -\psi_1(0)A + \psi_1(0)kln(-x) + \psi_1(0)k, \quad x < 0$$
$$\psi_1' = -\psi_1(0)B + \psi_1(0)kln(x) + \psi_1(0)k, \quad x > 0 \tag{8}$$

and $\psi_1'' = \psi_1(0)k/x$. Linear theory is obtained by matching these external solutions to solutions inside the resistive layer, which is considered infinitesimally thin. When the island becomes larger than the width of the resistive layer the solution is modified within the island and the matching must be done using the edges of the island r_l and r_r.

Growth is then given by $\Delta'(w)$ for width w with

$$\Delta'(w) = \frac{\psi_1'(x_r) - \psi_1'(x_l)}{\psi_1(0)} \simeq A - B + k[ln(x_r) - ln(-x_l)] \tag{9}$$

with subscripts r and l referring to the right and left edges of the island at the maximum width, $\theta = 0$, and $w = r_r - r_l$ is the island width. $\Delta'(w)$ describes the instantaneous growth rate and the magnetic energy of the island configuration, with $\Delta'(w) = 0$ at the magnetic energy minimum, the saturated state[10].

Again approximating the island width as narrow we have $\delta j_\phi \simeq \psi_1''$, and approximating $\psi_1'' = (\psi_1'(x_r) - \psi_1'(x_l))/w$, gives for the current due to the island perturbation

$$j_1(r,\theta) = \frac{\Delta'\psi_1}{w} cos(m\theta) \tag{10}$$

relating the current magnitude within the island to the stability.

The position of the island separatrix is determined by setting ψ to the value at the separatrix, given by the X-point, at $m\theta = \pi$ and approximately at $x = 0$, $\psi_s = \psi_0(0) - \psi_1(0)$. The edges x_l and x_r at $\theta = 0$ are determined by setting $\psi(r,0) = \psi_s$. Ordering terms in magnitude of ψ_1, the leading order gives

$$x_r = -x_l = \left(-\frac{4\psi_1(0)}{\psi_0''}\right)^{1/2} \tag{11}$$

so to this order the island is symmetric about the rational surface and the growth rate is given by

$$\Delta'(w) = A - B. \tag{12}$$

But as we will see, the island asymmetry is important, and local approximations not taking account of higher order terms give incorrect results.

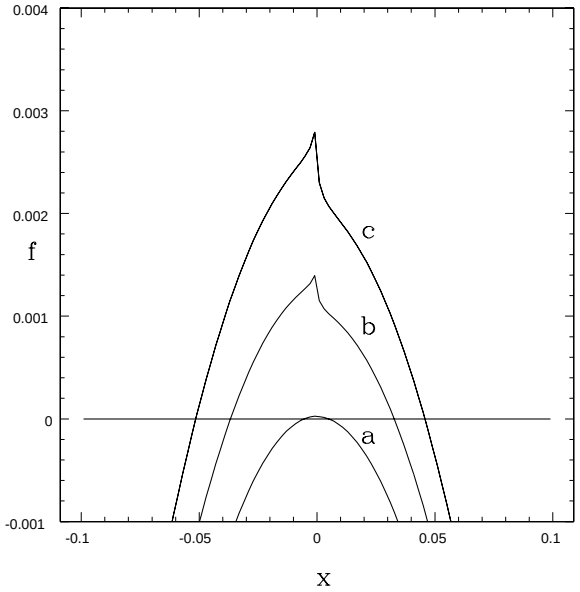

FIG. 3: Shift of X and O-points vs mode amplitude, with amplitudes of 10^{-6} (a), 5×10^{-5} (b), and 10^{-4} (c). The right zero corresponds to the location of the X-point, and the left zero that of the O-point.

O-point and X-point locations are at the local maxima in r of $\psi_0(r) + \psi_1(r)cos(m\theta)$, at $r > r_s$ for the X-point $cos(m\theta) = -1$ and at $r < r_s$ for the O-point $cos(m\theta) = 1$. The local expressions give for $r < r_s$

$$d\psi/dr = \psi_0'' x^2/2 + \alpha(A - kln(-x) - k) \tag{13}$$

and for $r > r_s$

$$d\psi/dr = \psi_0'' x^2/2 - \alpha(-B + kln(x) + k) \tag{14}$$

Solutions for $d\psi/dr = 0$ are shown in Fig. 3 for $\alpha = 10^{-6}$ (a), 5×10^{-5} (b), and 10^{-4} (c). Values of A and B were determined by a numerical integration of ψ_1. The O-point shift from $x = 0$ is generally larger than the X-point shift. This island asymmetry, due to the fact that ψ_1 is not constant across the island, was used in the analysis of tearing mode saturation[10].

III. CURRENT PERTURBATION

Now consider the effect on the island of current modifications within the island. The perturbed current density harmonic is given in the range $r_l < r < r_r$ by

$$\delta j_1(r) = \frac{1}{\pi}\int_0^{2\pi} d\theta cos(m\theta) j_I(\psi) \tag{15}$$

and $j_I(\psi)$ is a helically symmetric function of the island interior flux.

Using local expressions and taking flux surface averages at the hyperbolic and elliptic points[11] gives for the change in the growth rate of an island of width w due to perturbations of current δj_1 of

$$\frac{d\psi_1}{dt} = \frac{\eta(r_x)\Delta'(w)\psi_1}{w} - \eta(r_x)\delta j_1 \tag{16}$$

This equation involving islands with width larger than the tearing layer is known as the generalized Rutherford equation, first introduced in the analysis of tearing mode saturation[10]. The effect of the current perturbation is commonly expressed as a modification of Δ' by the addition of $\Delta'_{\delta j}$ with

$$\Delta'_{\delta j}(w) = -w\frac{\delta j_1}{\psi_1}, \tag{17}$$

and used for neoclassical bootstrap calculations and other effects[14–16]. Note that it is singular at zero island width.

Because of the island asymmetry $A = (r_r - r_x)/(r_x - r_l) - 1$, with r_x the X point location, there is a destabilizing effect producing a δj. In the island the flattening of the temperature profile and the resistivity leads to a flattening of the current profile, producing a perturbed negative current (destabilizing) for $r < r_x$ and a positive current perturbation (stabilizing) for $r > r_x$. Since temperature is equilibrated along the separatrix, and unless there is an imbalance between Ohmic heating and radiation loss it is constant across the island, the value of η and the magnitude of the current in the island are given by values at the X-point, so in the island $j = j(r_x)$. The effect of the asymmetry was noted in[17] with regard to the supression of the neoclassical tearing mode.

The modified current profile for large islands is shown schematically in black in Fig. 4. Aside from the fact that the heat flows through the X-point, thermically isolating the island, there are two additional effects analyzed by Fitzpatrick[1]. First, the diffusion modifies the

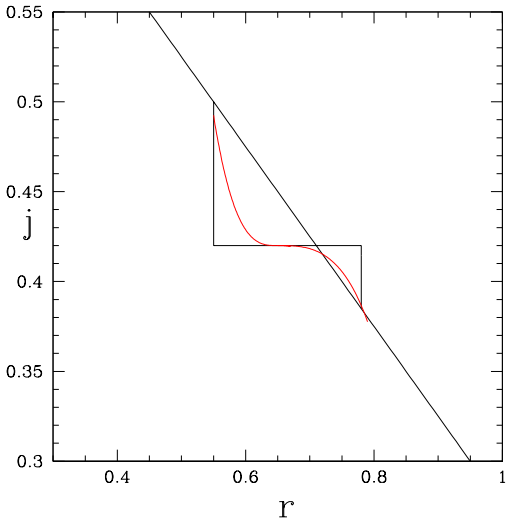

FIG. 4: Asymmetry of current profile flattening due to asymmetric island, producing a large negative current perturbation to the left of the rational surface and a smaller stabilizing current perturbation to the right of the rational surface. Schematic flattening is shown in black with the effect of thermal conductivity in red.

temperature and thus the current profile near the island edges for large islands. This is shown schematically in Fig. 4 in red. Simulations done in that work were for a symmetric slab geometry and flattening occured over a large fraction of the island interior. The effect on Δ' is given by the addition of Δ'_A with

$$\Delta'_A(w) = f_F \frac{\int [j(r_x) - j(r)] dr}{\psi_1(r_s)}, \tag{18}$$

where the subscript A is for asymmetry and $f_F < 1$ takes into account the degree of current profile flattening in the island. There are no results for the cylindrical case, so the degree of flattening has to be a free parameter in our model. The present analysis is incapable of determining the degree to which the current profile is flattened in the island, requiring a simulation which includes thermal transport. We have used values of f_F ranging from 0.5 to 1.0 with no change in the qualitative nature of the results.

Secondly, any modification of Δ' due to changes in the current profile in the island is not valid for very small island width, the perpendicular heat diffusion destroys the temperature perturbation and the normal equilibrium current profile is restored. The small island effect is expressed by multiplying $\Delta'_{\delta j}$ by $w^2/(w^2 + w_F^2)$, with w_F given by $\sqrt{8}(\kappa_\perp/\kappa_\parallel)^{1/4}(Rr_s/ns)^{1/2}$, where $s = r_s q'/q$ is the local shear and $\kappa_\perp$ and $\kappa_\parallel$ are the cross field and parallel heat

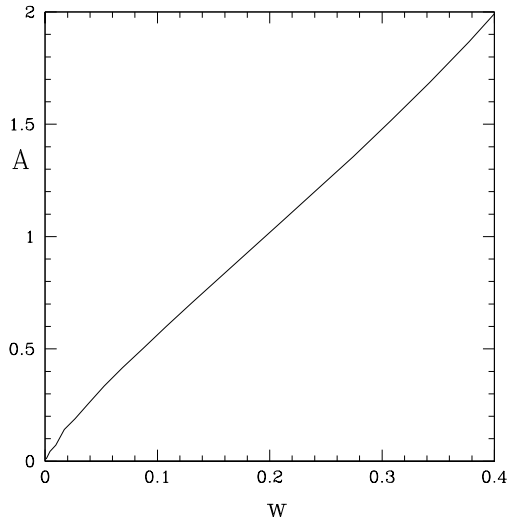

FIG. 5: Island asymmetry vs width.

conductivities. The same considerations apply to Δ'_A. For typical fusion plasma parameters $\kappa_\perp/\kappa_\| \sim 10^{-9}$ and with aspect ratio $R = 5$ we have $w_F \sim 0.02$.

Note that all previous calculations of tearing mode saturation did not allow for flattening of the current profile inside the island along with the asymmetry and thus did not include this effect.

Unlike the change in island width, the effective value of Δ' due to both effects can be found analytically using the local approximation. Including the Fitzpatrick factor for small islands we have

$$\Delta'_{\delta j}(w) = -\frac{32}{\pi}\frac{\delta j_1}{\psi''_0}\frac{w}{w^2+w_F^2}, \qquad \Delta'_A(w) = \frac{8j'(r_s)}{\pi\psi''_0}\frac{w^2}{w^2+w_F^2}f_A, \tag{19}$$

where f_A takes account of asymmetry A and degree of island flattening, given by $f_A = Af_F$, and a common factor of $2/\pi$ approximates the flux surface averaging. The analytic expression for the island width in terms of the amplitude, $4\sqrt{-\psi_1/\psi''_0}$ is fairly accurate, but the asymmetry and the saturated values of amplitude must be found numerically. We note that agreement with experimental values of neoclassical bootstrap current required increasing[14] the value of $\Delta'_{\delta j}$ above the analytic expression given by Eq. 19.

Shown in Fig. 5 is the asymmetry for the disruption case as a function of width w, seen to be almost linear in w, so f_A is approximately proportional to w. This linear dependence of the asymmetry on width is important for the temporal evolution of an island.

Shown in Fig. 6 are the island flux surfaces, in the state with $\Delta'(w)$ equal to zero[10]

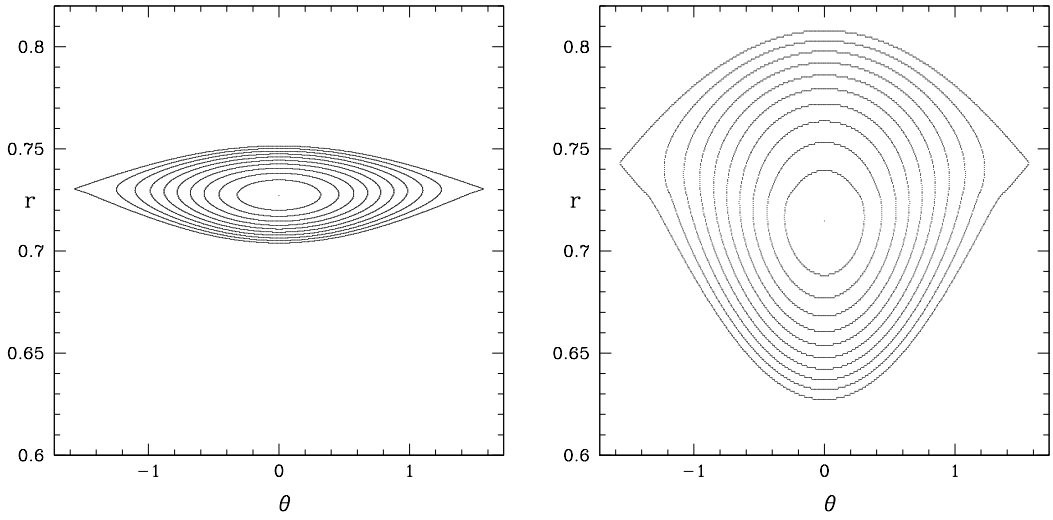

FIG. 6: Magnetic islands including the effect of current flattening. The small island has amplitude $\alpha = 10^{-4}$, and width $w = .05$, $A = .26$. The amplitude of the large island is $\alpha = 1.5 \times 10^{-3}$, with width $w = 0.18$, and asymmetry $A = .78$. Profile parameters are those of the disruption test case with $f_F = 1$.

with no current perturbation, with width $w = .05$ and asymetry $A = .26$, and a larger island due to a negative current perturbation with width $w = .18$ and asymmetry $A = .78$. The asymmetry and the shift of the X- and O-points are clearly visible in the larger island.

IV. ISLAND TEMPERATURE

Energy transport in the island is given by the balance of Ohmic heating and radiation

$$\partial_t E = \nabla \cdot (\kappa \nabla T) + H(T) - R(T) \tag{20}$$

with $H(T)$ the differential Ohmic heating and any other heating source in the island, and $R(T)$ the radiation loss, κ the cross field heat conductivity. We wish to find the steady state temperature profile in the island. Since in fusion plasmas the heat conductivity parallel to the magnetic field is typically nine orders of magnitude larger than the cross field conductivity we assume the temperature is equilibrated along the flux surfaces, so we require that $T = T(\psi)$. Then using $\nabla T = T' \nabla \psi$, and averaging $\partial_t E$ on the flux surfaces and setting it to zero we have

$$0 = \kappa T'' <(\nabla \psi)^2> + \kappa T' <(\nabla^2 \psi)> + H(T) - R(T) \tag{21}$$

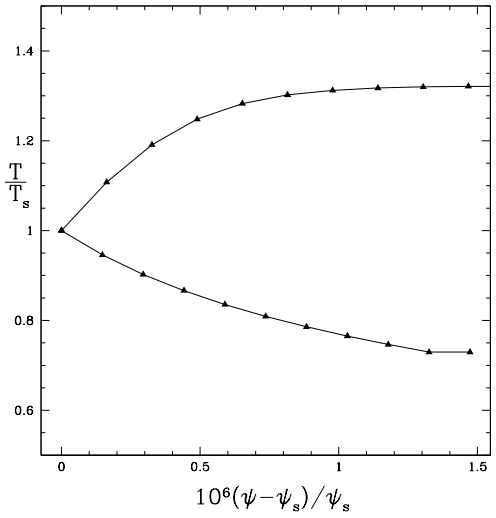

FIG. 7: Island temperature profiles for cases dominated by radiation and by Ohmic heating.

where the brackets indicate flux surface averaging. In the island $\nabla^2\psi \simeq \psi_0''(r_s)$ which is order one, and $(\nabla\psi)^2 \leq (\psi_0''(r_s)w)^2/4 << 1$, so in fact we are left with a first order differential equation for the temperature

$$0 = \kappa\psi_0''(r_s)\frac{dT}{d\psi} + H(T) - R(T) \tag{22}$$

with the boundary condition the value of T at the separatrix. With a balance between differential heating and radiative loss $dT/d\psi = 0$, the island temperature is everywhere equal to the value at the separatrix.

Examples of solutions $T(\psi)$ are shown in Fig. 7, where ad hoc functions for the Ohmic heating $H(T)$ and radiation $R(T)$ were used. The positive differential temperature case is dominated by Ohmic heating, and the negative differential temperature case by radiation. We used $\kappa = 1$, constant density, and $T = 1$ at the separatrix. These functions are simply to demonstrate the method of obtaining the temperature profile from the radiation and heating models, the shape does not reflect any physical model. From the change in T in the island interior we calculate the change in η and the subsequent change in the current profile in the island. Also from the temperature gradient in the island, the island width, and the local heat conductivity we can calculate the power necessary to obtain this temperature differential. A future publication will examine explicit models for radiation and heating including impurity and plasma density dependence[18] in order to make comparison with experiments.

The perturbed current harmonic resulting from Eq. 15 for the case of Spitzer resistivity

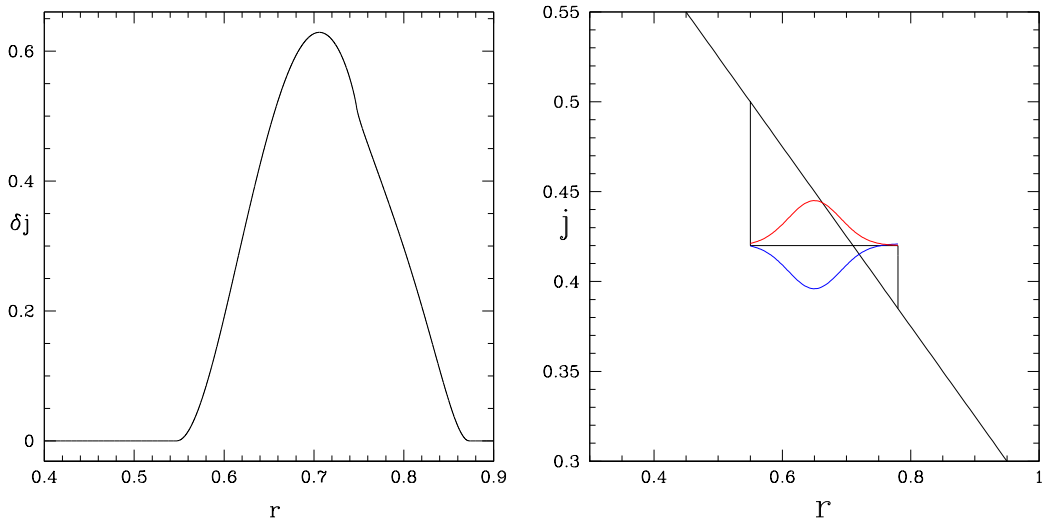

FIG. 8: Example of perturbed current harmonic $j_1(r)$. Spitzer resistivity $\delta j \sim T^{3/2}$ was used, with T linear in $\psi - \psi_s$ in the island interior. For this plot the magnitude of the perturbed current $j_I(\psi)$ was taken to be equal to the on-axis current density j_0. At the right is shown a schematic depiction of the two destabilizing effects. The asymmetry produces a large negative perturbation of $j(r)$ to the left of the rational surface and a smaller positive perturbation to the right. Excess radiation cooling over Ohmic heating produces a negative bulge of current in the center of the island, shown in blue, and heating produces a positive bulge, shown in red. Cooling and flattening are destabilizing and together produce exponential island growth.

$\eta \sim T^{-3/2}$ is shown in Fig. 8, with

$$j_I(\psi) = j_s \frac{T^{3/2}(\psi) - T_s^{3/2}}{T_s^{3/2}}, \tag{23}$$

and j_s and T_s the equilibrium current and termperature at the separatrix, and for this plot the temperature was taken to be a linear function of the flux in the island interior

Temporal evolution can be found by noting that when the island is larger than the tearing layer the growth is given by Eq. 16, or

$$\frac{dw}{dt} = r_s^2[\Delta'(w) + \Delta'_{\delta j}(w) + \Delta'_A(w)] \tag{24}$$

with time in units of the resistive time $\tau_R = r_s^2/\eta$.

It is easy to see that island heating causes saturation at small width, but an imbalance of radiation over Ohmic heating leads to exponential growth of the island. From Eq. 22

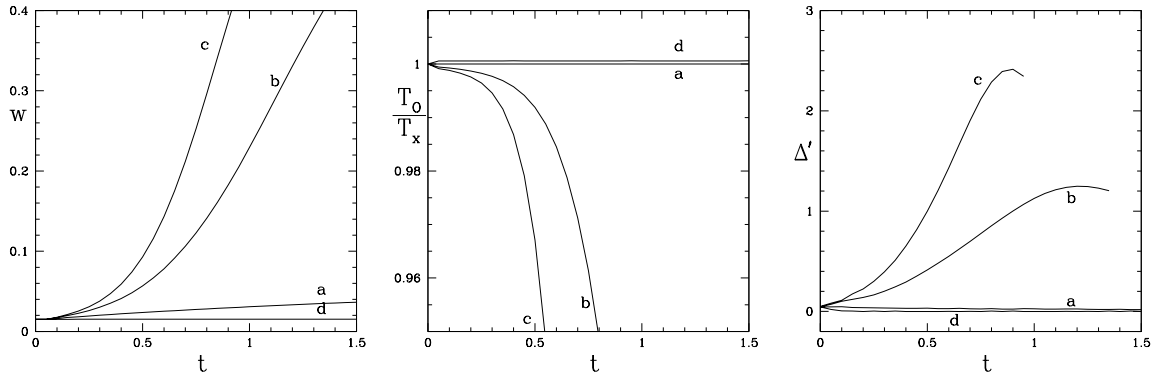

FIG. 9: Growth of an island in the disruption test equilibrium, with a fixed temperature gradient in the island, determined by an imbalance of radiation loss and Ohmic heating. Shown is the island width and the central temperature normalized to the temperature at the separatrix and Δ' at each time, giving the instantaneous island growth rate. Full flattening was assumed, $f_F = 1$. The plots are for a) radiation and heating balanced, b) and c) radiation dominated, d) heating dominated. At time $t = 0.2$ the imbalance produced an O-point temperature differential T_O/T_x of a) 0, b) -.002, c) -.003, and in the strongly cooled case (c) the temperature differential at t=0.5 with $w = 0.1$ was 3 percent. In the case with heating, (d) the final central island temperature differential was .001.

the temperature gradient in the island is fixed by the imbalance between radiation loss and Ohmic heating. Consider an initial state with a saturated island and introduce a constant radiation loss R. This will produce a negative temperature differential in the island interior with a peak value at the island O-point given by $Rd\psi \sim Rw^2$. The resistivity will increase and the current will decrease on a time scale for current diffusion producing a local perturbation of the current as shown in Fig. 8, proportional to w^2, giving a contribution to $\Delta'_{\delta j}(w)$ from Eq 19 proportional to w. In addition, since $f_A \sim w$, we find $\Delta'_A(w) \sim w$. The island grows with dw/dt proportional to w, ie exponentially. However, either one of these alone is not enough to produce exponential growth because of the stabilizing effect of $\Delta'(w)$.

In Fig. 9 are shown simulations of this process, with a small fixed imbalance between radiation loss and Ohmic heating. The initial state was given by a very small perturbation, producing a weakly unstable island with $w = 10^{-3}$. Time is in terms of the resistive time $\tau_R = r_s^2/\eta$. Each time step the mode amplitude is advanced using Eq. 24, the temperature integrated over the island flux surfaces, and δj_1 and $\Delta'(w)$, $\Delta'_{\delta j}(w)$, and $\Delta'_A(w)$ calculated.

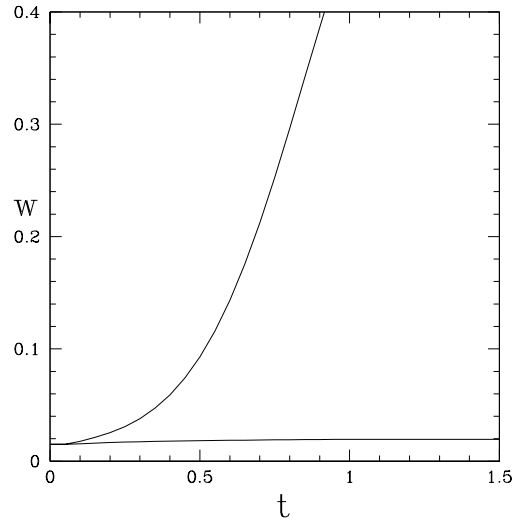

FIG. 10: Island evolution in the disruption case with and without the effect of asymmetric flattening. The radiation term is constant and the same for each case. Without the effect of asymmetric flattening exponential growth is absent, and the saturation width is much smaller than the case with flattening and no cooling.

Note that the temperature differential necessary to produce rapid growth is well below one percent for small island width, not easily noticable experimentally. Final island widths with heating of less than one percent are significantly smaller than unheated states.

Because of the strong effect of the asymmetry, unless the equilibrium is very near threshold, with Δ' small, island heating is necessary to maintain an island saturated at small width. Minimal cooling produces exponential growth. Without the effect of the flattening, cooling produces an increase in the saturated island width, but it takes a very extreme temperature differential to produce a large island. This is why previous attempts to describe the Greenwald effect through this process failed. An example of an initial perturbation near threshold with a small radiation term, with and without the effect of asymmetric flattening is shown in Fig. 10.

V. GENERAL EQUILIBRIA

In this section we explore a method of constructing a cylindrical equilibrium which best matches results for an equilibrium of general aspect ratio, shape, and beta. To do this we note that the island saturation dynamics is determined by the form of the helical flux

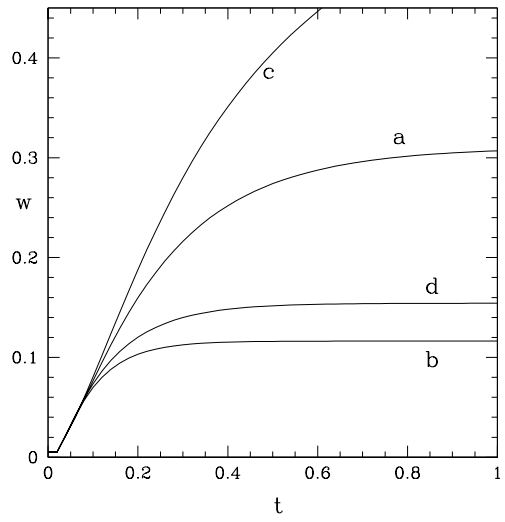

FIG. 11: Island evolution with the cylindrical formalism with and without the effect of asymmetric flattening of the current profile using equilibrium data from DEBS. a) flattening, no cooling, b) no cooling and no flattening, c) flattening with a small constant temperature gradient due to cooling, d) the same temperature gradient but no flattening. Without the effect of asymmetric flattening exponential growth is absent, and the saturation width is much smaller than the case with flattening and no cooling, only slightly larger than the case without flattening or cooling.

function, the current density profile and the q profile. Thus for any equilibrium we generate these functions of the outboard midplane minor radius, and then use this data to integrate the equations in the cylindrical model. The helical flux thus takes into account paramagnetic or diamagnetic modifications of the toroidal flux, and the current density profile and the q profile other modifications of the equilibrium from a large aspect ratio circular case.

This allows direct comparison with experimental equilibria, as well as with simulations using codes employing more general equilibria, including time evolution and heat transport, using the 3-D pressureless resistive compressible magtnetohydrodynamic (MHD) code DEBS[13], which includes an aspect ratio dependent paramagnetic modification of the toroidal field, changing the shape of the helical flux. In Fig. 11 is an example with the cylindrical analysis but using the q, j, and ψ profiles taken from a simulation with DEBS. The helicity profile ranged from $q(0) = 1.12$ to $q(1) = 3.4$, the rational surface was $r_s = .703$ and the aspect ratio $R/a = 2$. This equilibrium is more unstable to the $m = 2$ mode than the disruption case treated in the previous sections, so saturated island widths are signifi-

cantly larger. Simulations with DEBS must avoid the $q = 1$ surface for numerical reasons and shifting q upwards moved the equilibrium farther from threshold. The simulation with DEBS also gave unlimited growth of the island with a small imbalance of radiation over Ohmic heating, and the saturated island width with no curent flattening was in reasonable agreement with the cylindrical simulation shown above. More extensive results of the DEBS simulation are included[19] in a separate paper. Further simulations will be done also with the two fluid resistive MHD code NIMROD[20].

VI. CONCLUSIONS

From the analysis shown it is clear that the relative thermic isolation of a magnetic island and the effects of Ohmic heating and radiation can lead to rapid growth or mild contraction of a saturated island due to a tearing mode. The $m = 2$ island has long been a candidate for the onset of significant loss of plasma to the wall and the limiting or quenching of a discharge or even violent disruption[21]. In this paper we examine the destabilizing effect due to the asymmetry of the magnetic island, and show how relatively minor modification of the current profile in an island interior can lead to rapid change in the saturated island width, and that a dominant effect can be produced by temperature changes within the island. A small imbalance between radiation loss and Ohmic heating within an island can lead to rapid island growth. We also demonstrate how to solve for the temperature within the island due to the competing effects of Ohmic heating and radiation loss. Coupled with a model for radiation from the island interior due to density changes and influx of impurities this mechanism is a candidate for accounting for the Greenwald density limit. The inclusion of realistic models for radiation and plasma heating and thus dependencies on density and impurities will be included in future publications. In a full toroidal analysis toroidal coupling to higher harmonics would play an important role in leading to large scale stochastic fields and plasma loss, but this simple cylindrical treatment appears capable of demonstrating the major effects and allowing rapid exploration of a large range of equilibrium and radiation parameters. In addition it is capable of displaying qualitative effects due to the degree of current profile flattening in the island, the form of the radiation and Ohmic heating functions, modifications due to equilibrium changes due to plasma pressure and shape, etc. Future publications will make more detailed comparison of the cylindrical model with full

toroidal simulations, and explore a detailed comparison with the experimental Greenwald limit. It is also of interest to explore significance of this destabilizing effect on magnetic reconnection in the solar corona and in the magnetosphere.

Acknowledgement

This work was partially supported by the U.S. Department of Energy Grants DE-AC02-09CH11466.

---

[1] R. Fitzpatrick, Phys Plasmas 2, 825 (1995)

[2] E. Westerhof, A. Lazaros, E. Farshi, M.R. de Baar, M.F.M. de Bock, I.G.J. Classen, R.J.E. Jaspers, G.M.D. Hogeweij, H.R. Koslowski, A. Kramer-Flecken, Y. Liang, N.J. Lopes Cardoza and O. Zimmermann, Nucl. Fus. 47, 85 (2007)

[3] M. Greenwald, J. Terry, S. Wolfe, S. Ejima et al, Nuclear Fusion 28, 12, 2199 (1988)

[4] D.A. Gates and L. Delgado-Aparicio, Phys Rev. Lett. 108, 165004 (2012)

[5] P. H. Rebut and M. Hugon, "Thermal instability and disruptions in a tokamak", Plasma Physics and Controlled Nuclear Fusion Research 1984, Vol 2, IAEA-CN-44/E-III-7, IAEA Vienna (1985)

[6] F. Salzedes, F. C. Schiller, A. A. M. Oomens, Phys Rev. Lett. 88, 075002 (2002)

[7] D. A. Gates, B. Lloyd, A. W. Morris, G. McArdle, M. R. Obrien, M. Valovic, C. D. Warrick, H. R. R. Wilson, Compass-D team, ECRH team, Nuclear Fusion 37, 1593 (1997)

[8] D. A. Gates, L. Delgado-Aparicio, D. Brennan, R.B. White, Phys Rev. Lett. submitted (2014)

[9] H. P. Furth, P. H. Rutherford and H. Selberg, Phys Fluids 16, 1054 (1973)

[10] R. B. White, D. A. Monticello, M. N. Rosenbluth and B. V. Waddell, Phys Fluids 20, 800 (1977)

[11] R. B. White, *The Theory of Toroidally Confined Plasmas, third edition*, Imperial College Press, pp. 191, 352 (2014)

[12] P. H. Rutherford, Phys Fluids 16, 1903 (1973).

[13] D.D. Schnack, D.C. Barnes, Z. Mikic, D.S. Harned, E.J. Caramana, Jrnl. Comput. Phys. 70, 30 (1987)

[14] E. Fredrickson, M. Bell, R. V. Budny, and E. Synakowski, Phys of Plasmas 7, 4112 (2000)

[15] N. N. Gorelenkov, R V Budny, Z Chang, M V Gorelenkova, L E Zakharov, Physics of Plasmas,

Vol 3, Iss 9, pp 3379-3385 (1996)

[16] N. Bertelli, D. DeLazzari, and E. Westerhof, Nucl. Fus. 51, 103007 (2011)

[17] D. DeLazzari, and E. Westerhof, Plasma Phys. and Controlled Nuclear Fusion. 53, 135020 (2011)

[18] L. Delgado-Aparicio, D.A. Gates, Onset criteria for radiation- driven tearing modes, submitted (2014)

[19] D.P. Brennan, C. Liu, D.A. Gates, L. Delgado-Aparicio, and R. B. White, Simulation of explosive magnetic islands at the density limit, submitted (2014)

[20] D.D. Schnack, D.C. Barnes, Z. Mikic, D.S. Harned, E.J. Caramana, Jrnl. Comput. Phys. 140, 71 (1998), C.R. Sovinec, T.A. Granakon, E.D. Held, S.E. Kruger, D.D. Schnack, Phys Plas. 10, 1727 (2003)

[21] R. B. White, D. A. Monticello, M. N. Rosenbluth, Phys Rev. Lett 39, 1618 (1977)